

Electronic Supplementary Information

Morphological control of organic-inorganic perovskite layers by hot isostatic pressing for efficient planar solar cells

Toshinori Matsushima,^{*ab} Takashi Fujihara,^c Chuanjiang Qin,^{ab} Shinobu Terakawa,^a Yu Esaki,^a Sunbin Hwang,^{ad} Atula S. D. Sandanayaka,^{ab} William J. Potscavage, Jr.,^{ab} and Chihaya Adachi^{*abd}

^a Center for Organic Photonics and Electronics Research (OPERA), Kyushu University, 744 Motoooka, Nishi, Fukuoka 819-0395, Japan. E-mail: adachi@cstf.kyushu-u.ac.jp or tmatusim@opera.kyushu-u.ac.jp

^b JST, ERATO, Adachi Molecular Exciton Engineering Project, c/o Center for Organic Photonics and Electronics Research (OPERA), Kyushu University, 744 Motoooka, Nishi, Fukuoka 819-0395, Japan

^c Innovative Organic Device Laboratory, Institute of Systems, Information Technologies and Nanotechnologies (ISIT), 744 Motoooka, Nishi, Fukuoka 819-0395, Japan

^d International Institute for Carbon Neutral Energy Research (WPI-I2CNER), Kyushu University, 744 Motoooka, Nishi, Fukuoka 819-0395, Japan

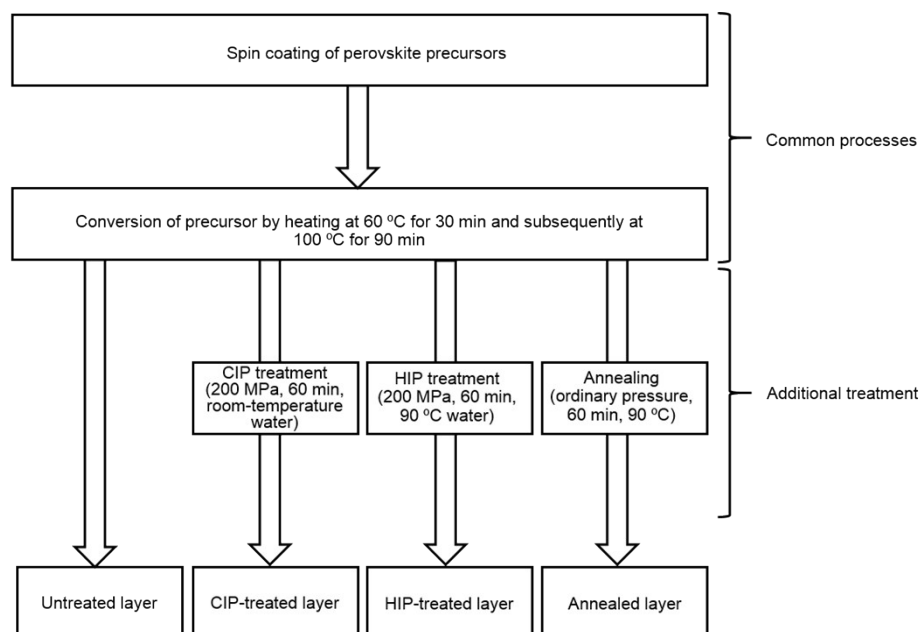


Fig. S1. Flowchart showing the perovskite layer fabrication and treatment processes. A precursor layer was spin-coated on PEDOT:PSS and then heated on a hot plate at 60 °C for 30 min and subsequently at 100 °C for 90 min to convert it to perovskite. These spin coating and heating processes, which are described in section 2.1, are common processes for all samples. The perovskite layers fabricated using only these common processes are termed untreated layers. Other perovskite layers were further treated with either CIP, HIP, or annealing (see the additional treatment processes in the flowchart and description in section 2.2).

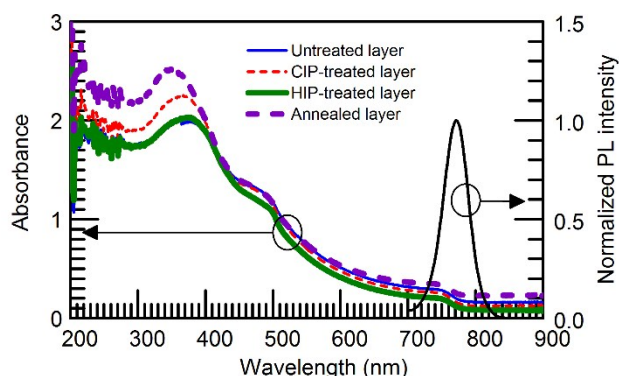


Fig. S2. UV-VIS-NIR absorption spectra of untreated, CIP-treated, HIP-treated, and annealed perovskite layers fabricated on fused silica substrates coated with PEDOT:PSS and a representative PL spectrum. Absorption of PEDOT:PSS is weak enough to be ignored. Absorbance at 850 nm is 0.161 for the untreated layer, 0.126 for the CIP-treated layer, 0.080 for the HIP-treated layer, and 0.229 for the annealed layer. Absorbance at 850 nm originates from light scattering by the roughness of the perovskite layers because this wavelength is beyond the absorption edge. Observed absorbance changes are well associated with morphological characteristics shown in Fig. 2. We assume that the absorption shapes are deformed by the presence of light scattering. The PL peak is located at around 770 nm near the absorption band edge.

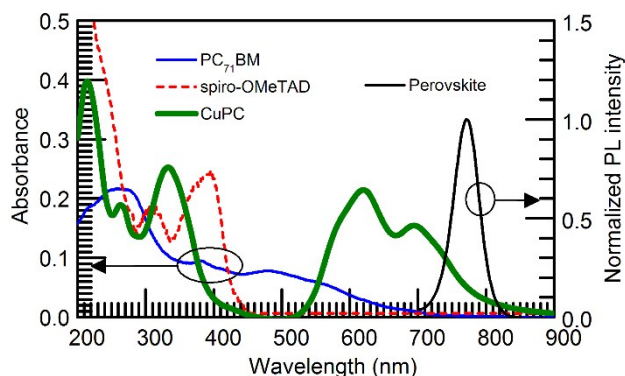


Fig. S3. UV-VIS-NIR absorption spectra of PC₇₁BM, spiro-OMeTAD, and CuPC layers fabricated on fused silica substrates and PL spectrum of perovskite. The perovskite/PC₇₁BM and perovskite/spiro-OMeTAD systems have no spectral overlap between absorption and PL, indicating that Förster type or Dexter type energy transfer should not influence the diffusion length estimated in this study. However, the presence of the spectral overlap for the perovskite/CuPC system can induce energy transfer between them to some extent.

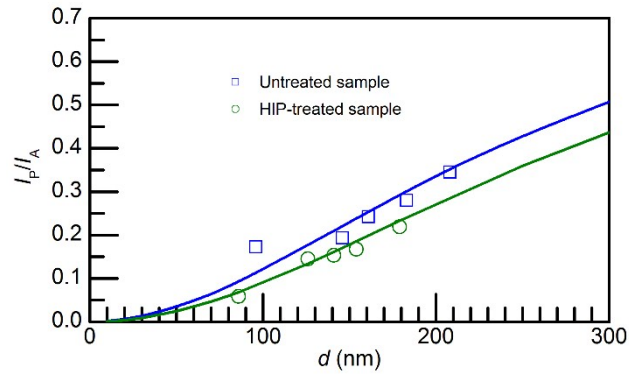


Fig. S4. I_p/I_A vs d plots of untreated and HIP-treated perovskite layers where CuPC was used as hole quencher. Symbols are experimental data. Solid curves are fitting results calculated using eqn (2). Fitting results in $L_h = 154 \pm 21$ nm for the untreated layers and $L_h = 182 \pm 13$ nm for the HIP-treated layers, which are similar to the values and trend measured using spiro-OMeTAD (Fig. 5b and Table 2). The energy transfer from the perovskite to CuPC seems to be negligible for the diffusion length calculation despite the presence of the spectral overlap shown in Fig. S2, probably because the energy transfer distance is much smaller than the perovskite thicknesses d .

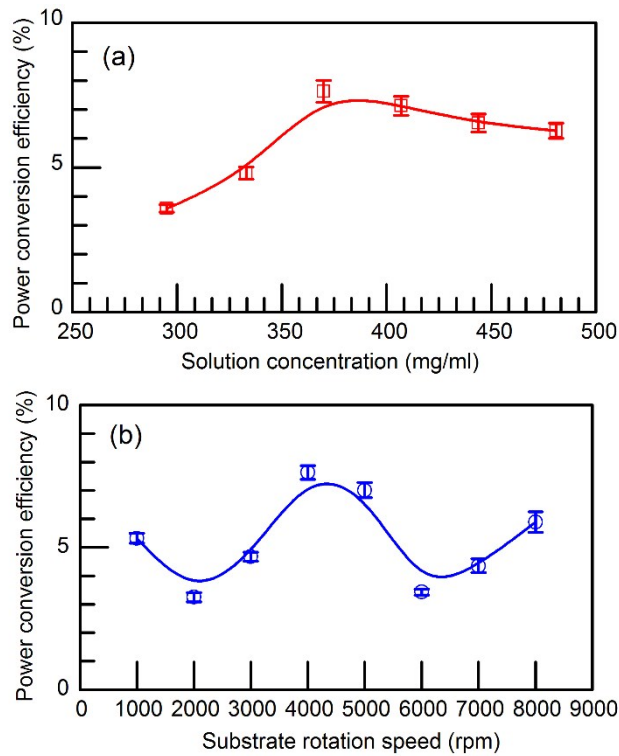


Fig. S5. Dependence of (a) solution concentrations and (b) substrate rotation speeds during perovskite spin coating on power conversion efficiencies of untreated perovskite solar cells. The solution concentration was varied from 295 to 481 mg ml⁻¹ at a constant substrate rotation speed of 4000 rpm, and the best efficiency was found for a concentration of 370 mg ml⁻¹. Next, the spin rate was varied from 1000 to 8000 rpm with a constant concentration of 370 mg ml⁻¹, and the optimized speed was found at 4000 rpm although (b) somewhat showed a “W” shape. Therefore, we used the conditions of 370 mg ml⁻¹ and 4000 rpm for the comparison of perovskite layer treatments.

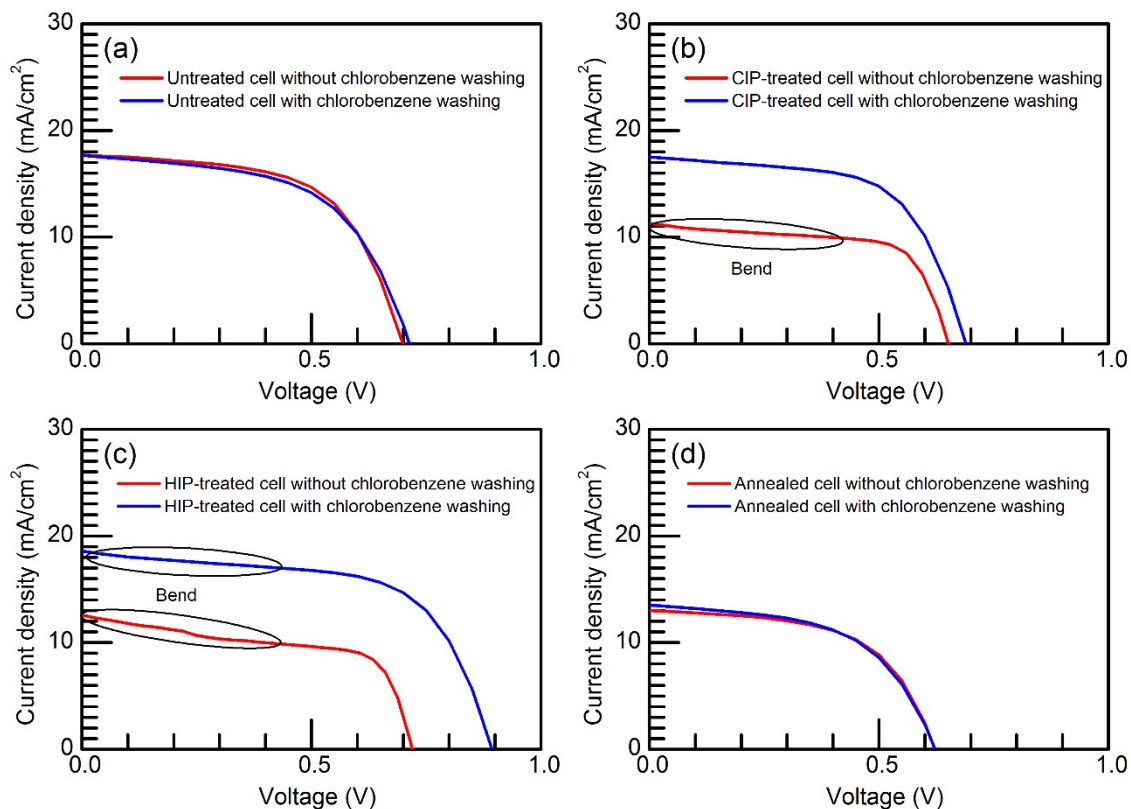


Fig. S6. Representative J - V curves of (a) untreated, (b) CIP-treated, (c) HIP-treated, and (d) annealed perovskite solar cells under simulated solar light (AM1.5G, 100 mW cm^{-2}) with and without washing of the perovskite layers by spin coating of chlorobenzene before cell fabrication. The CIP- and HIP-treated solar cells without chlorobenzene washing exhibited performance much worse than with washing and exhibited bends in their J - V curves in the 0-0.4 V region, probably because of contamination of the perovskite surfaces with impurities from the polymer bag during CIP and HIP treatments. Chlorobenzene washing resulted in an improvement in the solar cell performances for both the CIP- and HIP-treated cells and the nearly complete straightening of the J - V curves for CIP-treated cells while those of the HIP-treated cells retained a slight bend. The residual bend is because of incomplete removal of the impurities from the HIP-treated perovskite surfaces even after chlorobenzene washing. On the other hand, it was confirmed that chlorobenzene washing did not affect the performance of the untreated and annealed solar cells.